Effect of long-range interactions on multipartite entanglement in Heisenberg chains

Sudipto Singha Roy[1,2] and Himadri Shekhar Dhar[3,4]
[1]Instituto de Física Téorica UAM/CSIC, C/Nicolás Cabrera 13-15, Cantoblanco, 28049 Madrid, Spain
[2]Department of Applied Mathematics, Hanyang University (ERICA), 55 Hanyangdaehak-ro, Ansan, Gyeonggi-do 426-791, Korea
[3]Institute for Theoretical Physics, Vienna University of Technology, Wiedner Hauptstraße 8-10/136, 1040 Vienna, Austria
[4]Physics Department, Blackett Laboratory, Imperial College London, London SW7 2AZ, United Kingdom

(Received 1 October 2018; published 17 June 2019)

It is well known that the notions of spatial locality are often lost in quantum systems with long-range interactions, as exhibited by the emergence of phases with exotic long-range order and faster propagation of quantum correlations. We demonstrate here that such induced "quasinonlocal" effects do not necessarily translate to growth of global entanglement in the quantum system. By investigating the ground and quenched states of the variable-range, spin-1/2 Heisenberg Hamiltonian, we observe that the genuine multiparty entanglement in the system can either increase or counterintuitively diminish with a growing range of interactions. The behavior is reflective of the underlying phase structure of the quantum system and provides key insights for generation of multipartite entanglement in experimental atomic, molecular, and optical physics where such variable-range interactions have been implemented.

DOI: 10.1103/PhysRevA.99.062318

I. INTRODUCTION

In recent years, there has been considerable interest in investigating the physical properties related to quantum systems with long-range interactions [1–4]. This is primarily in response to the significant developments made in experimental atomic, molecular, and optical (AMO) physics [5–7], where such interactions can be implemented in a well-controlled setting [8–11]. These studies have led to a flurry of exciting new physical phenomena [12–26], for instance, propagation of correlations faster than the Lieb-Robinson bound [13–15], emergence of exotic long-range order [17–20], and dynamical phase transitions [21,22]. Most of these phenomena arise in the presence of long-range interactions due to the breakdown of "quasilocality" [27,28] (cf. [29]). In this context, quasilocality affirms the existence of a nonrelativistic spatial light cone within which most of the causal information travels with the finite Lieb-Robinson velocity [30]. Any correlations or response to local fluctuations appear to be strongly suppressed at small distances away from this light-cone boundary [31,32], which may not be the case when long-range interactions are present. Importantly, the loss of quasilocality can lead to nontrivial distribution of quantum entanglement [33], which over the years has been established as an important resource in implementation of various quantum information and computation protocols [34–36] (also see [37]). While recent studies have focused on the growth of entanglement between two parties in a variable-range interacting system [12,16], the effect of emergent quasinonlocality due to long-range interactions on the global entanglement of these systems remains elusive [38]. Here, we address this void by investigating the multipartite entanglement in the ground and quenched states of quantum many-body systems with long-range interactions.

It is known that entanglement jointly distributed among many parties has richer features [39,40], which has allowed for the design of sophisticated protocols such as cryptographic conference [41,42] and multiparty quantum communication [43–48]. Multiparty entangled states are also intrinsic resources in implementation of novel quantum computation models such as measurement-based quantum computation [49]. In the past decade, notable progress in experimental physics has allowed for the efficient creation and manipulation of multiparty entanglement [50–54]. This opens up the exciting potential for harnessing systems with a tunable range of interactions for physical realization of these quantum protocols. Moreover, multiparty entanglement is also an important characteristic quantity in the study of critical phenomena in many-body systems [55–62].

In this work, we consider a spin-1/2 Heisenberg chain with spin interactions that follow a power-law decay ($1/r^{\alpha}$). Efficient implementation of such variable interactions has been possible with recent developments in AMO physics, in particular with cold atoms [7], where the parameter α can be tuned. Other systems include Rydberg atoms [8], trapped ions [9], and polar molecules [10]. Incidentally, it is known that such power-law decay in the Heisenberg chain can lead to the breakdown of quasilocality [20,29]. An important ramification of this is that the area law no longer bounds the entanglement entropy [28] (cf. [63,64]), especially for $\alpha \leqslant 1$. In the same vein, intuitively, one would expect that the spatial nonlocal effects induced by the long-range interactions would result in quantum phases with enhanced global entanglement. To explore this further, we characterize the multiparty entanglement in both the ground and quenched states of the considered Hamiltonian. We observe a clear dichotomy between two different regimes, depending on whether the interactions in the x-y spin plane are antiferromagnetic (AFM) or ferromagnetic (FM). We note that while the ground states in the FM regime have enhanced multiparty entanglement for an increased range of interactions in the system, counterintuitively, for the AFM regime the global entanglement weakly diminishes. Interestingly, we note that this is no longer the case when quantum states are quenched with such long-range interactions. Here, we start from a completely separable or product spin state and switch on the interactions. The subsequent growth of multipartite entanglement in the time-evolved system is then numerically analyzed. Here, we observe that the AFM interactions with long range are more favorable towards the growth of multiparty entanglement, in contrast to the FM interactions, where the growth appears to be almost independent of the range of interactions. Thus, our findings clearly demonstrate that long-range interaction selectively enhances quantum resources, such as global entanglement in the system, and this is important for experimental efforts to generate entanglement and implement quantum information and computation protocols using systems with variable-range interactions.

This paper is arranged as follows. We introduce the spin-1/2 Heisenberg chain with long-range interactions in Sec. II. Our measure of genuine multipartite entanglement and its computation are discussed in Sec. III. In Sec. IV, we analyze the genuine multiparty entanglement in the ground states of the long-range model. The growth of entanglement under quantum quench is then investigated in Sec. V, before we end with a final discussion of the results in Sec. VI.

II. MODEL

We start by introducing the physical system of interest, the one-dimensional (1D) quantum spin lattice, consisting of spin-1/2 particles coupled via long-range interactions with power-law decay. The Heisenberg Hamiltonian governing such a system can be written as

$$\mathcal{H} = \sum_{i<j} \frac{1}{|i-j|^{\alpha}} \left(J_x \sigma_i^x \sigma_j^x + J_y \sigma_i^y \sigma_j^y + \Delta \sigma_i^z \sigma_j^z\right), \tag{1}$$

where $\alpha \geqslant 0$ is the continuous exponent that controls the long-range interaction. J_x and J_y are the coupling constants along the x and y spin axes, respectively, and Δ is the anisotropy along the z direction. Here, σ^m are the Pauli spin matrices ($m \in \{x, y, z\}$). For $J_x, J_y < 0$, the interaction in the x-y plane is ferromagnetic, while for $J_x, J_y > 0$, we obtain the antiferromagnetic coupling. The above Hamiltonian, in the presence of long-range interactions, has a rich phase diagram. For $J_x = J_y = -1$, an exotic continuous symmetry breaking (CSB) phase emerges [20] for low values of α, apart from the known XY and AFM phases observed in the short-range Hamiltonian. This is a true hallmark of the quasi-nonlocal effect and the change in effective dimensionality of the system induced by long-range interactions. This is due to the fact that spontaneous breaking of continuous symmetry typically appears only in higher-dimensional spin lattices and is otherwise forbidden in low-dimensional systems by the Mermin-Wagner theorem [65] (also see Ref. [20]). For $\alpha = \infty$, the model reduces to the short-range Heisenberg model with nearest-neighbor (NN) interactions. A schematic of a 1D long-range quantum spin system of arbitrary size and with power-law decay of interactions is provided in Fig. 1. In our study, we consider periodic boundary conditions for the spin

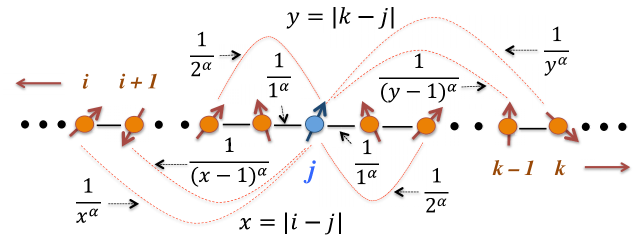

FIG. 1. Schematic of a quantum spin chain with interactions that follow a power-law decay, $1/r^{\alpha}$. The thick black and red dotted lines show the short- and long-range coupling between the jth and other spins in the quantum system.

chain. In order to do that we always choose the interaction corresponding to the shortest distance, $|i-j|$, from one site and another in the periodic spin chain. We note that at $\Delta = 0$, for $J_x = J_y$, the above Hamiltonian gives us the long-range XX model, which we analyze in our study. Moreover, for $\Delta = J_x = J_y$ and $\alpha = 2$, the model reduces to the exactly solvable Haldane-Shastry model [66–68].

III. MEASURE OF GENUINE MULTIPARTY ENTANGLEMENT

Before going into the detailed analysis of the entanglement properties of the ground and quenched states of the long-range Heisenberg model, we begin by defining the genuine multiparty entanglement of a quantum state. We note that there exists several equivalent definitions and measures of multiparty entanglement in the literature [33]. In our work, we are mainly focused on the genuine multiparty entanglement of a quantum system [69], which is defined as follows: An N-party pure quantum state $|\psi\rangle_N$ is said to be genuinely multiparty entangled if it cannot be written as a product in any bipartition. In other words, a genuine multiparty entangled state is entangled across all bipartitions of the system [70–72]. In order to estimate this quantity in $|\psi\rangle_N$, we consider the generalized geometric measure (GGM) [72], which is a computable measure of genuine multiparty entanglement of a state. It is defined as an optimized distance of the given quantum state $|\psi\rangle_N$ from the set of all states that are not genuinely multiparty entangled. This can be mathematically expressed as $\mathcal{G}(|\psi\rangle_N) = 1 - \Lambda^2_{\max}(|\psi\rangle_N)$, where $\Lambda_{\max}(|\psi\rangle_N) = \max |\langle\chi|\psi\rangle_N|$, with the maximization being over all such pure quantum state $|\chi\rangle$ that are not genuinely multiparty entangled. Following some simplifications, one can derive an equivalent expression for the above equation, given by [72]

$$\mathcal{G}(|\psi\rangle_N) = 1 - \max\left\{\lambda^2_{A:B} | A \cup B = \{s_1, \ldots, s_N\}, A \cap B = \emptyset\right\}, \tag{2}$$

where $\lambda_{A:B}$ is the maximal Schmidt coefficient of $|\psi\rangle_N$, in the bipartition $A : B$. The measure is then optimized over all possible bipartitions of the state $|\psi\rangle_N$ and, for spin-1/2 or qubit systems, takes values in the range $0 \leqslant \mathcal{G}(|\psi\rangle_N) \leqslant 1/2$. In recent years, GGM has been used to characterize genuine multiparty entanglement in strongly correlated systems, including quantum spin liquids [73,74], doped spin lattices [75,76], and other many-body systems [77–81].

We note that the computation of GGM in many-body quantum systems requires access to the complete state of the system and all its reduced density matrices. In general, for a quantum system with N sites, the number of such reduced density matrices is given by $\sum_{i=1}^{N/2}\binom{N}{i}$, which increases exponentially with the size of the system. Moreover, in the presence of long-range interactions, there are no known analytical or approximate methods, such as tensor networks or matrix product states, which can be used to compute GGM, as is the case in several short-range models (see Refs. [73–75,82]). Therefore, in our case, we are restricted to exact numerical solutions for small, finite-spin chains. In our work, we have considered systems with up to $N = 20$ spins and use diagonalization and propagation methods based on the Krylov subspace and Lanczos algorithm. To mitigate the effect of unstable finite-size effects in the presence of long-range interactions, we have also checked the qualitative consistency of our main results against smaller system sizes.

IV. MULTIPARTY ENTANGLEMENT IN THE GROUND STATE

We now study the variation of genuine multiparty entanglement $\mathcal{G}$ in the ground states of the spin-1/2 Heisenberg chain with long-range interactions, given by Eq. (1). Towards that aim, we consider two distinct regimes emanating from the Hamiltonian, (i) the ferromagnetic regime, with interactions in the x-y plane given by $J_x = J_y = -1$, and (ii) the antiferromagnetic regime, with $J_x = J_y = 1$. Here, we consider only the antiferromagnetic interactions along the z axis, i.e., $0 \leqslant \Delta/J \leqslant 2$ ($J = |J_x| = |J_y|$), where there always exists a distinct gap between the lowest-energy values. The long-range interaction in the system is controlled through the exponent α, which is varied in the integer range $1 \leqslant \alpha \leqslant 10$. We exclude the extreme points corresponding to systems with infinite interactions ($\alpha = 0$) or strictly NN interactions ($\alpha = \infty$).

We start with the FM regime and consider the case where the interaction is defined by $\alpha = 10$, with variable anisotropy between the x-y and z directions. We note that the system is already short range for $\alpha = 10$. In Fig. 2, we note that the ground state is genuinely multiparty entangled for all values of the anisotropy parameter Δ/J ($0 \leqslant \Delta/J \leqslant 2$), with the minimum $\mathcal{G}$ at the point $\Delta/J = 1$. As the range of interaction is increased, by decreasing α, the genuine multipartite entanglement increases monotonically for $\Delta/J < 1$. Subsequently, at higher values of anisotropy ($\Delta/J > 1$) the local minimum shifts to larger values of Δ/J for decreasing values of α. Moreover, there is a crossover between $\mathcal{G}$ values of different α, which gives rise to an interesting regime where the shortest range ($\alpha = 10$) and the longest range of interactions ($\alpha = 1$) generate ground states with higher global entanglement than the intermediate range of interactions. More importantly, $\mathcal{G}$ remains the highest at $\alpha = 1$ and gradually decreases with increasing Δ. Therefore, as long-range interactions in the system increase, there is an expected hike in the genuine multipartite entanglement in the ground state of the ferromagnetic spin-1/2 Heisenberg Hamiltonian.

In the AFM regime, the situation is drastically different. For the short-range interaction ($\alpha = 10$), the genuine multiparty entanglement of the ground state is the minimum at

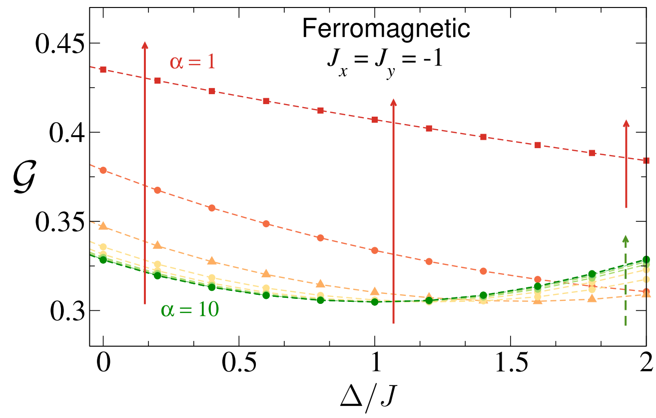

FIG. 2. Variation of genuine multipartite entanglement. Here, we consider a Heisenberg chain with $N = 20$ spins and FM interactions ($J_x = J_y = -1$) in the x-y plane. The plot shows the variation in $\mathcal{G}$ with the parameter Δ/J, where $J = |J_x| = |J_y|$, for ten different integer values of the exponent α, ranging from $\alpha = 1$ (red squares) to $\alpha = 10$ (green circles). Here, the dashed lines are fits to the plotted data points. The regime $\Delta = 0$ corresponds to the XX model, which also mimics the result obtained for the Heisenberg chain at low Δ. We note that the plots for higher α values are very close together, which shows that the short-range character is reached fairly quickly. Moreover, the solid red vertical arrows highlight specific parameter regimes where $\mathcal{G}$ increases with decreasing α (or increasing long-range interactions), whereas the dashed green vertical arrows show regions where $\mathcal{G}$ increases, but now for increasing α (or decreasing long-range interactions). Both the axes are dimensionless.

$\Delta/J = 1$, with a distinct symmetry around the point, as shown in Fig. 3. In contrast to the FM regime, $\Delta/J = 1$ is the local minimum of $\mathcal{G}$ for all values of α, although in the vicinity of this point the multipartite entanglement increases for more long-range interactions, which is similar to the FM regime.

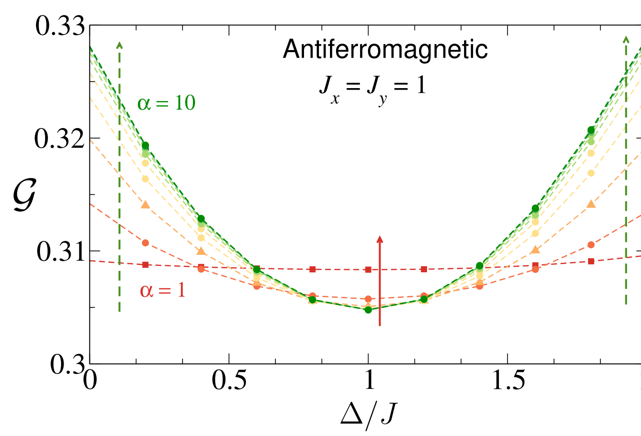

FIG. 3. Variation of genuine multipartite entanglement. Here, we consider a Heisenberg chain with $N = 20$ spins and AFM interactions ($J_x = J_y = 1$) in the x-y plane. The plot shows the variation in $\mathcal{G}$ with the parameter Δ/J (where $J = |J_x| = |J_y|$) for ten different integer values of the exponent α, ranging from $\alpha = 1$ (red squares) to $\alpha = 10$ (green circles). Once more, the dashed lines are just fits to the plotted data points, and both axes here are dimensionless. The red and green vertical arrows here imply the same behavior as outlined in Fig. 2.

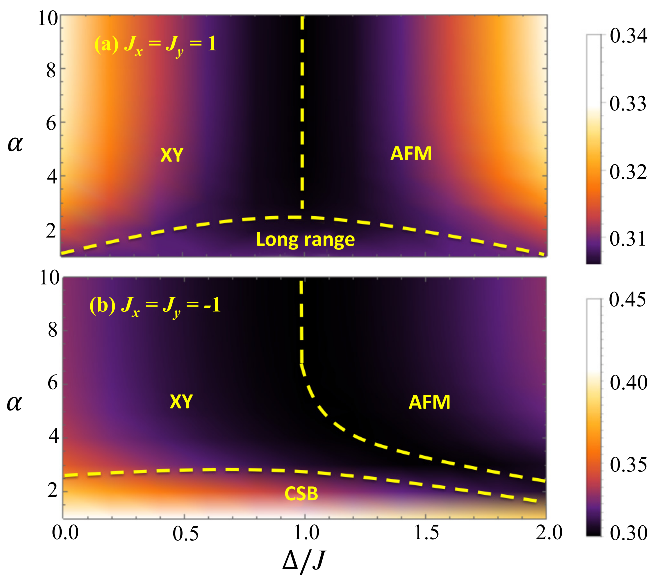

FIG. 4. Variation of genuine multiparty entanglement $\mathcal{G}$ in the ground states of the long-range Heisenberg chain consisting of $N = 20$ spins in the Δ/J-α plane for (a) AFM and (b) FM interactions in the x-y plane. Here, $J = |J_x| = |J_y|$. We note here that the dashed yellow lines represent the extremal (minima) points of $\mathcal{G}$. However, they serve only as a visual aid to deconstruct the known quantum phases of the model (see Ref. [20]). Both the axes and the color bar are dimensionless.

However, away from this point, $\mathcal{G}$ decreases as the long-range interaction in the system is increased. This intriguing behavior of genuine multipartite entanglement is in direct contrast to the behavior of the system in the FM regime and implies a negative interdependence between global entanglement and long-range-induced nonlocal effects in the system. This is significant from the perspective of physical implementation of quantum protocols where multiparty entanglement is an important resource. In the AFM regime, long-range interactions appear to be detrimental to generating large entangled states, compared to the FM regime.

The difference in the behavior of the genuine multipartite entanglement between the FM and AFM regimes can be partly explained using a heuristic description of the ground state in these regimes based on our numerical simulations. Here, the competition between different ground-state configurations in interacting many-body systems gives rise to the phenomenon of entanglement frustration [83] (also see Refs. [61,79]), which can potentially define the complex behavior of entanglement in our model. In the long-range interaction model that we consider, the ground state can be written as a superposition between two stable, but competing, configurations, such that $|\psi_g\rangle = a\,|\psi_{\rm N}\rangle + b\,|\phi_{\bar{\rm N}}\rangle$. Here, $|\psi_{\rm N}\rangle$ is the state arising due to the Néel order at $\Delta > 1$ (for $J = 1$). It is expected that at large Δ, the ground state will be closer to the Néel state for both the AFM and FM models. For large α, this is simply given by $|\psi\rangle = |\uparrow\downarrow\uparrow\cdots\downarrow\rangle$, where $\{\uparrow,\downarrow\}$ are the eigenstates of σ_z. However, the complementary configuration $|\psi'\rangle = |\downarrow\uparrow\downarrow\cdots\uparrow\rangle$ is also a likely ground state at large Δ. Hence, at dominant Δ values, frustration ensures that $|\psi_{\rm N}\rangle = \beta_1|\psi\rangle + \beta_2|\psi'\rangle$. The parity symmetry of $\mathcal{H}$ results in $\beta_1 = \pm\beta_2 = 1/\sqrt{2}$, which ensures $|\psi_{\rm N}\rangle$ is maximally multiparty entangled. On the other hand, $|\phi_{\bar{\rm N}}\rangle$ refers primarily to the non-Néel configurations in the ground state, which are orthogonal to both $|\psi\rangle$ and $|\psi'\rangle$. These states are significant in regimes where Δ is not large and seem to arise from the XY terms in the Hamiltonian. However, unlike $|\psi_{\rm N}\rangle$, the entanglement properties of $|\phi_{\rm N}\rangle$ are *a priori* not known.

While the above description is intuitively appealing for regimes that correspond to either large or small values of the anisotropy parameter, numerical analysis suggests that it can also provide a broad picture of the ground state for intermediate values of Δ. By investigating the quantum fidelity of the ground state to $|\psi\rangle$ and $|\psi'\rangle$, one can deduce that the overall entanglement of the ground state is dependent on the trade-off between the states $|\psi_{\rm N}\rangle$ and $|\phi_{\bar{\rm N}}\rangle$, i.e., the ratio a/b. In the AFM case, two distinct regimes emerge for all α, symmetric around the point $\Delta = 1$, viz., the region with $a > b$ (for $\Delta > 1$) and the one with $b > a$ (for $\Delta < 1$). We call these the Néel and non-Néel regimes. Later, we discuss how these regimes closely correspond to the AFM and XY phases, respectively. In the Néel regime, we observe that the ratio a/b increases not only with Δ but also with α, resulting in higher entanglement for shorter-range interactions. Interestingly, in the non-Néel regime the opposite behavior is observed. Here, it can be numerically shown that the ratio b/a increases for decreasing Δ values, resulting in more entanglement close to $\Delta = 0$. However, b/a also increases with increasing α, which again leads to higher entanglement in short-range systems. This allows a distinct symmetry in multiparty entanglement to emerge around the vicinity of $\Delta = 1$ (in the region, $0 \leqslant \Delta \leqslant 2$) for all values of α in the AFM model, but with short-range interactions leading to more entanglement, as shown in Fig. 3. Things look more interesting in the FM case, where the effects of long-range interactions become more prominent. First, for $\alpha > 1$, the transition from the Néel to the non-Néel regime is no longer centered at $\Delta = 1$, apart from the short-range cases ($\alpha > 6$). The different points of transition on Δ increase for decreasing α. This allows for crossover between the multiparty entanglement corresponding to different values of α. Second, more importantly, there is no Néel to non-Néel transition for $\alpha = 1$ in the FM case, at least within the considered parameter regime. Therefore, the ground state always corresponds to high values of b/a (in the non-Néel regime) and has high multiparty entanglement compared to other values of α (see Fig. 2).

Incidentally, we note that in the short-range limit (i.e., $\alpha = 10$), due to the SU(2) invariance of the Hamiltonian, the AFM and FM model turns out to be the same at $\Delta = \pm 1$. Moreover, in the short-range limit, the FM and AFM models here are also connected via local unitary operations (spin-flip operations at alternate sites in the spin chain) that keep the global entanglement unchanged. This is reflected in Figs. 2 and 3, where the plots for multiparty entanglement $\mathcal{G}$ at $\alpha = 10$ are almost the same for both the FM and AFM cases.

The dichotomy in the behavior of genuine multipartite entanglement in the ground state of the FM and AFM regimes of the Heisenberg Hamiltonian is closely related to their respective phase structures. In Fig. 4, we show that the genuine multipartite entanglement is able to deconstruct the different phases in these regimes, as has been established in earlier work [20]. For large α, the phases are similar to their counterparts corresponding to the NN spin-1/2 Heisenberg chain, with two distinct phases: the *XY* spin liquid phase and the AFM Ising-like phase. Figures 4(a) and 4(b) show how $\mathcal{G}$ distinctly highlights these phases in both the AFM and FM regimes, respectively. We note that the ferromagnetic phase corresponding to $\Delta < -1$ is not shown in the diagram, as $\mathcal{G}$ cannot be uniquely computed for degenerate ground states. The anomalous behavior arises as α is decreased and one enters the quasinonlocal regime. For the AFM case, a regime of a relatively weak entangled phase appears, with lower values of $\mathcal{G}$. In contrast, in the FM regime, the continuous-symmetry-breaking phase emerges with decreasing α ($\alpha \lesssim 2$) [20], which is marked by a region of high genuine multiparty entanglement. Therefore, in terms of the phase diagram, the increase in genuine multipartite entanglement with increasing long-range interactions is related to the *XY*-CSB phase transition in the FM regime. In addition to this, at the truly long range interaction limit ($\alpha \sim 1$), the ground state mostly remains in the CSB phase, which apparently does not decrease quickly even when the anisotropy and Néel order increase with Δ.

V. GENERATING ENTANGLEMENT THROUGH QUANTUM QUENCH

We now look at how genuine multipartite entanglement can be generated through a quantum quench mediated by the variable-range interactions in either the FM or AFM regime of the spin Hamiltonian. In particular, we start with a product or completely separable initial state of the system, given by $|\psi\rangle_{in} = \prod_i^N |\phi\rangle_i$, where $|\phi\rangle_i = \frac{1}{\sqrt{2}}(|0\rangle_i + |1\rangle_i)$. Here, $|0\rangle_i$ and $|1\rangle_i$ are the eigenstates of σ_i^z. The initial states here can be thought to be ground states of some local Hamiltonian acting identically on all the spins. For the quantum quench, the long-range interactions are instantaneously switched on in the spin system. Subsequently, the initially separable quantum state rapidly evolves in time, leading to potential growth of multiparty entanglement in the system. We note that the quench performed in our study is motivated from the perspective of various quantum information and computation protocols, where entanglement is necessary for successful implementation of the protocol. To this end, in our quench process we begin with a completely separable product state, which is a resourceless state, and wish to generate a useful resource (entanglement) in the system. Our main aim here is to see whether the presence of long-range interactions in the Heisenberg Hamiltonian can generate higher entanglement or a quantum resource in these quenched states compared to a process that invokes only short-range interactions during the quench.

The initial state is subjected to a quantum quench and coherently evolves to $|\psi(t)\rangle = \exp(-i\mathcal{H}t)|\psi\rangle_{in}$. Subsequently, we measure how much GGM is generated in the quenched state; that is, we calculate $\mathcal{G}(|\psi(t)\rangle)$. We are interested in the parameter regimes away from $\Delta = 1$, where the dichotomy between the ground states in the FM and AFM cases appears to be the most distinct. Figure 5 shows the evolution of the state after the quench. Surprisingly, for the quenched

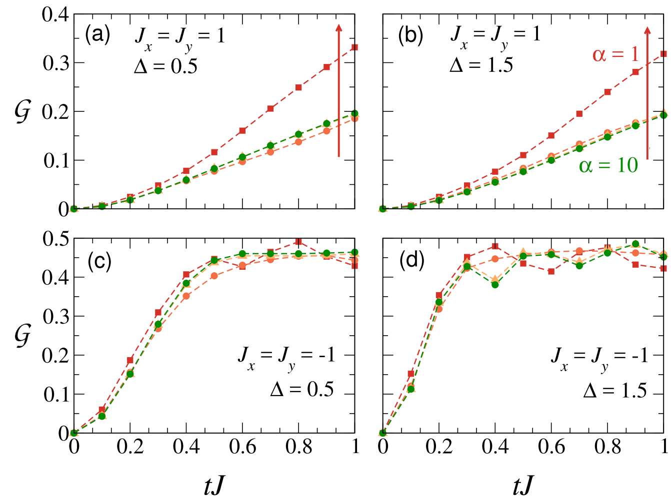

FIG. 5. Genuine multiparty entanglement after a quantum quench. The growth of $\mathcal{G}$ in a system consisting of $N = 12$ spins after a quantum quench of the initially product state $|\psi\rangle_{in}$ for (a) and (b) AFM and (c) and (d) FM interactions in the x-y plane. Here, $J = |J_x| = |J_y|$, and the plots correspond to $\alpha = 1$ (red squares), 2 (green circles), 5 (yellow triangles), and 10 (orange circles). The red vertical arrow here implies the same behavior as outlined in Fig. 2. The axes are all dimensionless.

dynamics, long-range interactions ($\alpha = 1$) appear to play a strong role in the growth of multipartite entanglement when $|\psi\rangle_{in}$ is quenched in the AFM regime. In contrast, the generation of multipartite entanglement in the FM regime is almost independent of the range of interactions in the system. This implies that highly entangled quantum states can be generated through quenching in the FM regime even in the absence of any significant long-range interactions. Therefore, in quenched dynamics long-range interactions seem to affect the multiparty entanglement favorably in the AFM regime, while remaining ambivalent in the FM regime. This is the converse to the outcome that was observed in the ground-state phases of the system.

VI. DISCUSSION

In this work, we have demonstrated how the quasinonlocal effect induced by long-range interactions in many-body systems selectively affects the multipartite entanglement of the system. By investigating different ground-state phases of the spin-1/2 Heisenberg Hamiltonian we observed that multiparty entanglement can be enhanced or, counterintuitively, can decrease as the range of interactions is increased. In particular, these opposing effects were observed for two distinct ground-state phases depending on whether the interaction in the x-y plane was ferromagnetic or antiferromagnetic. While the global entanglement is expectedly boosted with more quasinonlocal effects for the FM regime, in contrast, long-range interactions appear to act detrimentally in the AFM case. A possible reason for the unexpected behavior in the AFM regime, as we observed in our ground-state analysis, is the entanglement frustration arising from Néel and non-Néel terms, which appears to favor more global entanglement in the short-range limit. In the FM case, no transition occurs between the Néel and non-Néel regimes for long-range interactions, leading to higher entanglement.

Interestingly, the observed dichotomy in these regimes was intriguingly different while considering the generation of multiparty entanglement through quenched dynamics of initially separable states. Here, long-range interactions allow for robust growth of global entanglement in the AFM regime, in contrast to the FM regime, where there is no perceptible advantage in using longer interactions in the quenched dynamics. Overall, our results clearly demonstrate that the system in the ferromagnetic interaction regime is more susceptible to allowing significant global entanglement for both short- and long-range interactions.

Our findings provide significant insights for physical implementation of quantum protocols where multiparty entanglement is a necessary resource, such as measurement-based computation and secure multiparty communication. With recent technological breakthroughs in experimental atomic, molecular, and optical physics, where the systems often contain tunable long-range interactions, it is essential to determine the optimal range of interactions that will allow for maximal global entanglement in these system, which can then be harnessed in the quantum protocol.

ACKNOWLEDGMENTS

The authors thank R. Fazio for useful discussions at ICTP, Trieste. H.S.D. acknowledges funding from the Austrian Science Fund (FWF), Project No. M 2022-N27, under the Lise Meitner program of the FWF.

[1] T. Lahaye, C. Menotti, L. Santos, M. Lewenstein, and T. Pfau, The physics of dipolar bosonic quantum gases, Rep. Prog. Phys. **72**, 126401 (2009).

[2] D. Peter, S. Müller, S. Wessel, and H. P. Büchler, Anomalous Behavior of Spin Systems with Dipolar Interactions, Phys. Rev. Lett. **109**, 025303 (2012).

[3] Z.-X. Gong, M. F. Maghrebi, A. Hu, M. Foss-Feig, P. Richerme, C. Monroe, and A. V. Gorshkov, Kaleidoscope of quantum phases in a long-range interacting spin-1 chain, Phys. Rev. B **93**, 205115 (2016).

[4] J. Zeiher, J.-y. Choi, A. Rubio-Abadal, T. Pohl, R. van Bijnen, I. Bloch, and C. Gross, Coherent Many-Body Spin Dynamics in a Long-Range Interacting Ising Chain, Phys. Rev. X **7**, 041063 (2017).

[5] I. Bloch, J. Dalibard, and W. Zwerger, Many-body physics with ultracold gases, Rev. Mod. Phys. **80**, 885 (2008).

[6] M. Saffman, T. G. Walker, and K. Mølmer, Quantum information with Rydberg atoms, Rev. Mod. Phys. **82**, 2313 (2010).

[7] J. S. Douglas, H. Habibian, C.-L. Hung, A. V. Gorshkov, H. J. Kimble, and D. E. Chang, Quantum many-body models with cold atoms coupled to photonic crystals, Nat. Photonics **9**, 326 (2015).

[8] P. Schauß, M. Cheneau, M. Endres, T. Fukuhara, S. Hild, A. Omran, T. Pohl, C. Gross, S. Kuhr, and I. Bloch, Observation of spatially ordered structures in a two-dimensional Rydberg gas, Nature (London) **491**, 87 (2012).

[9] J. W. Britton, B. C. Sawyer, A. C. Keith, C. C. J. Wang, J. K. Freericks, H. Uys, M. J. Biercuk, and J. J. Bollinger, Engineered two-dimensional Ising interactions in a trapped-ion quantum simulator with hundreds of spins, Nature (London) **484**, 489 (2012).

[10] B. Yan, S. A. Moses, B. Gadway, J. P. Covey, K. R. A. Hazzard, A. M. Rey, D. S. Jin, and J. Ye, Observation of dipolar spin-exchange interactions with lattice-confined polar molecules, Nature (London) **501**, 521 (2013).

[11] R. Islam, C. Senko, W. C. Campbell, S. Korenblit, J. Smith, A. Lee, E. E. Edwards, C.-C. J. Wang, J. K. Freericks, and C. Monroe, Emergence and frustration of magnetism with variable-range interactions in a quantum simulator, Science **340**, 583 (2013).

[12] J. Schachenmayer, B. P. Lanyon, C. F. Roos, and A. J. Daley, Entanglement Growth in Quench Dynamics with Variable Range Interactions, Phys. Rev. X **3**, 031015 (2013).

[13] P. Hauke and L. Tagliacozzo, Spread of Correlations in Long-Range Interacting Quantum Systems, Phys. Rev. Lett. **111**, 207202 (2013).

[14] P. Richerme, Z.-X. Gong, A. Lee, C. Senko, J. Smith, M. Foss-Feig, S. Michalakis, A. V. Gorshkov, and C. Monroe, Non-local propagation of correlations in quantum systems with long-range interactions, Nature (London) **511**, 198 (2014).

[15] P. Jurcevic, B. P. Lanyon, P. Hauke, C. Hempel, P. Zoller, R. Blatt, and C. F. Roos, Non-local propagation of correlations in quantum systems with long-range interactions, Nature (London) **511**, 202 (2014).

[16] A. S. Buyskikh, M. Fagotti, J. Schachenmayer, F. Essler, and A. J. Daley, Entanglement growth and correlation spreading with variable-range interactions in spin and fermionic tunneling models, Phys. Rev. A **93**, 053620 (2016).

[17] P. Bruno, Absence of Spontaneous Magnetic Order at Nonzero Temperature in One- and Two-Dimensional Heisenberg and *XY* Systems with Long-Range Interactions, Phys. Rev. Lett. **87**, 137203 (2001).

[18] N. Laflorencie, I. Affleck, and M. Berciu, Critical phenomena and quantum phase transition in long range Heisenberg antiferromagnetic chains, J. Stat. Mech. (2005) P12001.

[19] A. M. Lobos, M. Tezuka, and A. M. García-García, Restoring phase coherence in a one-dimensional superconductor using power-law electron hopping, Phys. Rev. B **88**, 134506 (2013).

[20] M. F. Maghrebi, Z.-X. Gong, and A. V. Gorshkov, Continuous Symmetry Breaking in 1D Long-Range Interacting Quantum Systems, Phys. Rev. Lett. **119**, 023001 (2017).

[21] B. Sciolla and G. Biroli, Dynamical transitions and quantum quenches in mean-field models, J. Stat. Mech. (2011) P11003.

[22] B. Žunkovič, M. Heyl, M. Knap, and A. Silva, Dynamical Quantum Phase Transitions in Spin Chains with Long-Range Interactions: Merging Different Concepts of Nonequilibrium Criticality, Phys. Rev. Lett. **120**, 130601 (2018).

[23] J. Smith, A. Lee, P. Richerme, B. Neyenhuis, P. W. Hess, P. Hauke, M. Heyl, D. A. Huse, and C. Monroe, Many-body

localization in a quantum simulator with programmable random disorder, Nat. Phys. **12**, 907 (2016).

[24] D. Jaschke, K. Maeda, J. D. Whalen, M. L. Wall, and L. D. Carr, Critical phenomena and Kibble-Zurek scaling in the long-range quantum Ising chain, New J. Phys. **19**, 033032 (2017).

[25] B. Neyenhuis, J. Zhang, P. W. Hess, J. Smith, A. C. Lee, P. Richerme, Z.-X. Gong, A. V. Gorshkov, and C. Monroe, Observation of prethermalization in long-range interacting spin chains, Sci. Adv. **3**, 1700672 (2017).

[26] Z. Eldredge, Z.-X. Gong, J. T. Young, A. H. Moosavian, M. Foss-Feig, and A. V. Gorshkov, Fast Quantum State Transfer and Entanglement Renormalization Using Long-Range Interactions, Phys. Rev. Lett. **119**, 170503 (2017).

[27] J. Eisert, M. van den Worm, S. R. Manmana, and M. Kastner, Breakdown of Quasilocality in Long-Range Quantum Lattice Models, Phys. Rev. Lett. **111**, 260401 (2013).

[28] Z.-X. Gong, M. Foss-Feig, F. G. S. L. Brandão, and A. V. Gorshkov, Entanglement Area Laws for Long-Range Interacting Systems, Phys. Rev. Lett. **119**, 050501 (2017).

[29] D. J. Luitz and Y. Bar Lev, Emergent locality in systems with power-law interactions, Phys. Rev. A **99**, 010105(R) (2019).

[30] E. Lieb and D. Robinson, The finite group velocity of quantum spin systems, Commun. Math. Phys. **28**, 251 (1972).

[31] M. Hastings and T. Koma, Spectral gap and exponential decay of correlations, Commun. Math. Phys. **256**, 781 (2006).

[32] B. Nachtergaele and R. Sims, Lieb-Robinson bounds and the exponential clustering theorem, Commun. Math. Phys. **265**, 119 (2006).

[33] R. Horodecki, P. Horodecki, M. Horodecki, and K. Horodecki, Quantum entanglement, Rev. Mod. Phys. **81**, 865 (2009).

[34] A. K. Ekert, Quantum Cryptography Based on Bell's Theorem, Phys. Rev. Lett. **67**, 661 (1991).

[35] C. H. Bennett and S. J. Wiesner, Communication Via One- and Two-Particle Operators on Einstein-Podolsky-Rosen States, Phys. Rev. Lett. **69**, 2881 (1992).

[36] C. H. Bennett, G. Brassard, C. Crepeau, R. Jozsa, A. Peres and W. K. Wooters, Teleporting an Unknown Quantum State Via Dual Classical and Einstein-Podolsky-Rosen Channels, Phys. Rev. Lett. **70**, 1895 (1993).

[37] M. A. Nielsen and I. Chuang, *Quantum Computation and Quantum Communication* (Cambridge University Press, Cambridge, 2000).

[38] S. Pappalardi, A. Russomanno, B. Žunkovič, F. Iemini, A. Silva, and R. Fazio, Scrambling and entanglement spreading in long-range spin chains, Phys. Rev. B **98**, 134303 (2018).

[39] G. Vidal, W. Dür, and J. I. Cirac, Reversible Combination of Inequivalent Kinds of Multipartite Entanglement, Phys. Rev. Lett. **85**, 658 (2000).

[40] F. Verstraete, J. Dehaene, B. De Moor, and H. Verschelde, Four qubits can be entangled in nine different ways, Phys. Rev. A **65**, 052112 (2002).

[41] S. J. D. Phoenix, S. M. Barnett, P. D. Townsend, and K. J. Blow, Multi-user quantum cryptography on optical networks, J. Mod. Opt. **42**, 1155 (1995); P. D. Townsend, Quantum cryptography on multiuser optical fibre networks, Nature (London) **385**, 47 (1997).

[42] S. Bose, V. Vedral, and P. L. Knight, Multiparticle generalization of entanglement swapping, Phys. Rev. A **57**, 822 (1998).

[43] A. Karlsson and M. Bourennane, Quantum teleportation using three-particle entanglement, Phys. Rev. A **58**, 4394 (1998).

[44] S. Bandyopadhyay, Teleportation and secret sharing with pure entangled states, Phys. Rev. A **62**, 012308 (2000).

[45] G. Rigolin, Quantum teleportation of an arbitrary two-qubit state and its relation to multipartite entanglement, Phys. Rev. A **71**, 032303 (2005).

[46] Y. Yeo and W. K. Chua, Teleportation and Dense Coding with Genuine Multipartite Entanglement, Phys. Rev. Lett. **96**, 060502 (2006).

[47] P. Agrawal and A. Pati, Perfect teleportation and superdense coding with W states, Phys. Rev. A **74**, 062320 (2006).

[48] S. Ghose and A. Hamel, Quantum communication using a multiqubit entangled channel, in *Women in Physics: 5th IUPAP International Conference on Women in Physics*, AIP Conf. Proc. No. 1697 (AIP, New York, 2016), p. 070002.

[49] R. Raussendorf and H. J. Briegel, A One-Way Quantum Computer, Phys. Rev. Lett. **86**, 5188 (2001).

[50] M. Eibl, N. Kiesel, M. Bourennane, C. Kurtsiefer, and H. Weinfurter, Experimental Realization of a Three-Qubit Entangled W State, Phys. Rev. Lett. **92**, 077901 (2004).

[51] R. Prevedel, G. Cronenberg, M. S. Tame, M. Paternostro, P. Walther, M. S. Kim, and A. Zeilinger, Experimental Realization of Dicke States of up to Six Qubits for Multiparty Quantum Networking, Phys. Rev. Lett. **103**, 020503 (2009).

[52] W. B. Gao, C. Y. Lu, X. C. Yao, P. Xu, O. Gühne, A. Goebel, Y. A. Chen, C. Z. Peng, Z. B. Chen, and J. W. Pan, Experimental demonstration of a hyper-entangled ten-qubit Schrödinger cat state, Nat. Phys. **6**, 331 (2010).

[53] J.-W. Pan, Z.-B. Chen, C.-Y. Lu, H. Weinfurter, A. Zeilinger, and M. Żukowski, Multiphoton entanglement and interferometry, Rev. Mod. Phys. **84**, 777 (2012).

[54] X. C. Yao, T. X. Wang, P. Xu, H. Lu, G. S. Pan, X. H. Bao, C. Z. Peng, C. Y. Lu, Y. A. Chen, and J. W. Pan, Observation of eight-photon entanglement, Nat. Photonics **6**, 225 (2012).

[55] T.-C. Wei, D. Das, S. Mukhopadyay, S. Vishveshwara, and P. M. Goldbart, Global entanglement and quantum criticality in spin chains, Phys. Rev. A **71**, 060305(R) (2005).

[56] H. T. Cui, Multiparticle entanglement in the Lipkin-Meshkov-Glick model, Phys. Rev. A **77**, 052105 (2008).

[57] R. Orús, Universal Geometric Entanglement Close to Quantum Phase Transitions, Phys. Rev. Lett. **100**, 130502 (2008).

[58] S. M. Giampaolo and B. C. Hiesmayr, Genuine multipartite entanglement in the XY model, Phys. Rev. A **88**, 052305 (2013).

[59] J. Stasińska, B. Rogers, M. Paternostro, G. De Chiara, and A. Sanpera, Long-range multipartite entanglement close to a first-order quantum phase transition, Phys. Rev. A **89**, 032330 (2014).

[60] M. Hofmann, A. Osterloh, and O. Gühne, Scaling of genuine multiparticle entanglement close to a quantum phase transition, Phys. Rev. B **89**, 134101 (2014).

[61] S. S. Roy, H. S. Dhar, D. Rakshit, A. Sen(De), and U. Sen, Detecting phase boundaries of quantum spin-1/2 XXZ ladder via bipartite and multipartite entanglement transitions, J. Magn. Magn. Mater. **444**, 227 (2017).

[62] L. Pezzé, M. Gabbrielli, L. Lepori, and A. Smerzi, Multipartite Entanglement in Topological Quantum Phases, Phys. Rev. Lett. **119**, 250401 (2017).

[63] M. B. Hastings, An area law for one-dimensional quantum systems, J. Stat. Mech. (2007) P08024.

[64] J. Eisert, M. Cramer, and M. B. Plenio, Area laws for the entanglement entropy, Rev. Mod. Phys. **82**, 277 (2010).

[65] N. D. Mermin and H. Wagner, Absence of Ferromagnetism or Antiferromagnetism in One- or Two-Dimensional Isotropic Heisenberg Models, Phys. Rev. Lett. **17**, 1133 (1966).

[66] B. S. Shastry, Exact Solution of an $S = 1/2$ Heisenberg Antiferromagnetic Chain with Long-Ranged Interactions, Phys. Rev. Lett. **60**, 639 (1988).

[67] F. D. Haldane, Exact Jastrow-Gutzwiller Resonating-Valence-Bond Ground State of the Spin-1/2 Antiferromagnetic Heisenberg Chain with $1/r^2$ Exchange, Phys. Rev. Lett. **60**, 635 (1988).

[68] M. Gaudiano, O. Osenda, and G. A. Raggio, Two-spin-subsystem entanglement in spin-1/2 rings with long-range interactions, Phys. Rev. A **77**, 022109 (2008)

[69] G. D. Chiara and A. Sanpera, Genuine quantum correlations in quantum many-body systems: A review of recent progress, Rep. Prog. Phys. **81**, 074002 (2018).

[70] T. C. Wei and P. M. Goldbart, Geometric measure of entanglement and applications to bipartite and multipartite quantum states, Phys. Rev. A **68**, 042307 (2003).

[71] M. Blasone, F. Dell'Anno, S. De Siena, and F. Illuminati, Hierarchies of geometric entanglement, Phys. Rev. A **77**, 062304 (2008).

[72] A. Sen(De) and U. Sen, Channel capacities versus entanglement measures in multiparty quantum states, Phys. Rev. A **81**, 012308 (2010); Bound genuine multisite entanglement: Detector of gapless-gapped quantum transitions in frustrated systems, arXiv:1002.1253.

[73] H. S. Dhar, A. Sen(De), and U. Sen, Characterizing Genuine Multisite Entanglement in Isotropic Spin Lattices, Phys. Rev. Lett. **111**, 070501 (2013); The density matrix recursion method: Genuine multisite entanglement distinguishes odd from even quantum spin ladder states, New J. Phys. **15**, 013043 (2013).

[74] S. S. Roy, H. S. Dhar, D. Rakshit, A. Sen(De), and U. Sen, Diverging scaling with converging multisite entanglement in odd and even quantum Heisenberg ladders, New J. Phys. **18**, 023025 (2016).

[75] S. S. Roy, H. S. Dhar, D. Rakshit, A. Sen(De), and U. Sen, Analytical recursive method to ascertain multisite entanglement in doped quantum spin ladders, Phys. Rev. B **96**, 075143 (2017).

[76] S. Das, S. S. Roy, H. S. Dhar, D. Rakshit, A. Sen(De), and U. Sen, Adiabatic freezing of entanglement with insertion of defects in a one-dimensional Hubbard model, Phys. Rev. B **98**, 125125 (2018).

[77] R. Prabhu, S. Pradhan, A. Sen(De), and U. Sen, Disorder overtakes order in information concentration over quantum networks, Phys. Rev. A **84**, 042334 (2011).

[78] A. Biswas, R. Prabhu, A. Sen(De), and U. Sen, Genuine-multipartite-entanglement trends in gapless-to-gapped transitions of quantum spin systems, Phys. Rev. A **90**, 032301 (2014).

[79] L. Jindal, A. D. Rane, H. S. Dhar, A. Sen(De), and U. Sen, Patterns of genuine multipartite entanglement in frustrated quantum spin systems, Phys. Rev. A **89**, 012316 (2014).

[80] U. Mishra, D. Rakshit, R. Prabhu, A. Sen(De), and U. Sen, Constructive interference between disordered couplings enhances multiparty entanglement in quantum Heisenberg spin glass models, New J. Phys. **18**, 083044 (2016).

[81] D. Sadhukhan, S. S. Roy, A. K. Pal, D. Rakshit, A. Sen(De), and U. Sen, Multipartite entanglement accumulation in quantum states: Localizable generalized geometric measure, Phys. Rev. A **95**, 022301 (2017).

[82] S. S. Roy, H. S. Dhar, A. Sen(De), and U. Sen, Tensor-network approach to compute genuine multisite entanglement in infinite quantum spin chains, Phys. Rev. A **99**, 062305 (2019).

[83] C. M. Dawson and M. A. Nielsen, Frustration, interaction strength, and ground-state entanglement in complex quantum systems, Phys. Rev. A **69**, 052316 (2004).